

## N O T I C E

THIS DOCUMENT HAS BEEN REPRODUCED FROM  
MICROFICHE. ALTHOUGH IT IS RECOGNIZED THAT  
CERTAIN PORTIONS ARE ILLEGIBLE, IT IS BEING RELEASED  
IN THE INTEREST OF MAKING AVAILABLE AS MUCH  
INFORMATION AS POSSIBLE

# NASA Technical Memorandum 82737

(NASA-TM-82737) ELUCIDATION OF WEAR  
MECHANISMS BY FERROGRAPHIC ANALYSIS (NASA)  
18 p HC A02/MF A01 CSCL 20K

N82-15199

Unclas  
G3/27 08756

## Elucidation of Wear Mechanisms by Ferrographic Analysis

**William R. Jones, Jr.**  
*Lewis Research Center*  
*Cleveland, Ohio*

Prepared for the  
Technical Symposium on Water-Glycol Hydraulic Fluids  
sponsored by BASF Wyandotte Corporation  
Wyandotte, Michigan, October 8, 1981



**NASA**

# ELUCIDATION OF WEAR MECHANISMS BY FERROGRAPHIC ANALYSIS

by William R. Jones, Jr.

National Aeronautics and Space Administration  
Lewis Research Center  
Cleveland, Ohio 44135

## ABSTRACT

The use of Ferrographic analysis in conjunction with light and scanning electron microscopy is described for the elucidation of wear mechanisms taking place in operating equipment. Examples of adhesive wear, abrasive wear, corrosive wear, rolling element fatigue, lubricant breakdown, and other wear modes are illustrated. In addition, the use of magnetic solutions to precipitate nonmagnetic debris from aqueous and nonaqueous fluids is described.

## INTRODUCTION

The advent of modern surface tools (refs. 1 and 2) and methods of lubricant analysis (refs. 3-5) affords the tribologist great flexibility in studying and monitoring lubrication problems. However, this dazzling array of techniques (table 1) can inundate a prospective user with a mountain of information. In addition, many of these techniques require very specialized equipment, highly trained operators, and someone to interpret the final results. Some of the devices would also require disassembly of the machine in order to examine the wearing part. This paper describes a method of combining three of the techniques (light microscopy, scanning electron microscopy and Ferrography) for the elucidation of wear mechanisms in an operating piece of machinery.

## APPARATUS

### Light Microscope

The microscope used in this study is a Richert Zetopan large research microscope equipped with a bichromatic illumination system, a camera and a photodetector. The bichromatic system is illustrated in figure 1. The system provides for both transmitted green light and reflected red light simultaneously. This high contrast combination makes it possible to distinguish light transmitted through particles from light reflected by the surfaces of the particles. Opaque particles return the reflected light and appear red. Transparent particles reflect little light but pass the transmitted light and appear green. The microscope is also equipped with polarizers which allow examination of particles in reflected polarized light. This yields information concerning the optical activities of the particles. The photodetector is used to measure the amount of particles at various locations on a Ferrogram.

## Scanning Electron Microscope (SEM)

The SEM used in this study is an ISI-40/4 having a 60 Å resolution with 10 X to 600 000 X magnification range. In addition, the system is equipped with a PGT SYSTEM III energy dispersive x-ray analyzer for elemental particle analysis.

### Ferrograph

The Ferrograph (refs. 6 and 7) is an instrument used to magnetically precipitate wear particles from a used oil onto a specially prepared glass slide. A mixture of 3 ml of used oil and 1 ml of solvent is prepared. This mixture is then slowly pumped over the slide as shown in figure 2. A solvent wash and fixing cycle follows which removes residual oil and permanently attaches the particles to the slide. The resulting slide with its associated particles is called a Ferrogram. A sketch of a Ferrogram slide is illustrated in figure 3.

## CLASSIFICATION OF WEAR PARTICLES

### Adhesive Wear Particles (Normal Rubbing Wear)

This ubiquitous wear particle is present in almost all oil samples, regardless of source. This flake-like particle, which is typically 0.75 to 1  $\mu\text{m}$  in thickness for steel surfaces, is generated during sliding. The major dimension is usually less than 15  $\mu\text{m}$ . An example of this type of wear debris is shown in the scanning electron micrograph (fig. 4) of a Ferrogram from elastohydrodynamic experiments (ref. 8). Normally, these particles are arranged in strings by the magnetic field of the Ferrograph (fig. 5).

This particle type is generated from a thin surface layer that is continuously formed during the sliding process. The particles are released into the lubricant by an exfoliation or fatigue-like process. An example of this layer on a wear scar from a boundary lubrication study (ref. 9) is shown in figure 6. Normally, the rate of removal of this layer is less than its rate of formation. Wear will continuously occur but usually at a low rate. Therefore, the presence of adhesive or normal rubbing wear particles in a lubricant usually indicates that a benign wear mode is operative.

If this surface layer is removed more rapidly than it can reform (due to either high loads or high speeds) more severe wear modes will occur. In fact, three high wear regimes have been identified for sliding steel surfaces before catastrophic failure occurs (ref. 10). As the severity of wear increases, larger and larger free metal particles are produced, then red oxides ( $\text{Fe}_2\text{O}_3$ ), black oxides ( $\text{Fe}_3\text{O}_4$ ), and finally massive free metal particles are formed at failure.

### Abrasive Wear

Abrasive or cutting wear occurs when a hard surface or a hard particle abrades a softer surface. The particles formed are very similar to those produced by a lathe, only on a microscale. Typically, these particles are 2-5  $\mu\text{m}$  wide and 25-100  $\mu\text{m}$  long. Examples of this wear particle type are illustrated in figure 7.

The presence of abrasive contaminants or abrasive wear debris in a lubrication system may cause the generation of much finer (thicknesses to 0.25  $\mu\text{m}$ ) wire-like debris (ref. 11). In any case, the occurrence of abrasive wear debris indicates an abnormal wear mode. Their quantity should be carefully monitored.

### Rolling Element Fatigue

Rolling element bearings generate three distinct particle types related to fatigue. First, fatigue spall fragments are observed. This is the material released when a spall opens up. Typically, these particles are flat, irregularly shaped, platelets initially up to 100  $\mu\text{m}$  in size. They have a major dimension to thickness ratio of about 10 to 1. In many respects, these particles are similar in morphology to normal rubbing wear particles, only larger. Examples of this type particle appear in figure 8.

Particles thought to be related to rolling element fatigue are metallic microspheres. They resemble miniature ball bearings and are on the order of 1 to 5  $\mu\text{m}$  in diameter. Presumably, they are generated in propagating fatigue cracks (ref. 12). When these cracks reach the surface, spheres are released into the oil when about 60 percent of the fatigue life of the bearing has elapsed. Our work (fig. 9) has shown an increase in sphere count just prior to failure as detected by accelerometers (ref. 13). These increases occurred at greater than 95 percent of the bearing lives. Earlier work (ref. 14) involving accelerated rolling element fatigue tests yielded mixed results. Some tests yielded increases in sphere counts while in others few spheres were detected (fig. 10). An example of a sphere from a rolling element fatigue test appears in figure 11.

A third particle type is sometimes observed during rolling element fatigue. These are large (20-50  $\mu\text{m}$  in major dimension) laminar particles having a thickness ratio of about 30 to 1. They are probably formed by the passage of a wear particle through a rolling contact.

### Severe Wear Particles

Severe wear particles encompass debris from a variety of wear processes. As the name implies, when these particles are observed, a severe or perhaps fatal wear mode is taking place. In general, these particles can be identified by size alone (i.e., > 20  $\mu\text{m}$  in major dimension). Their surfaces often show signs of excessive surface heating or tearing. An example of such a particle appears in figure 12.

### Iron Oxide Particles

Occasionally, because of water contamination or other reasons, a spectrometer oil analysis (SOAP) will indicate large quantities of iron in a lubricant. However, after precipitation by the Ferrograph, it is evident that most of the iron is in the form of oxides or rust (fig. 13). This condition, which should be rectified, is not nearly as serious as one in which all of the iron would be in the form of wear debris.

## Nonferrous Particles

Nonferrous particles often appear in oil samples. They are the result of wear processes taking place in pumps, hydraulic system components, bearings or other parts containing nonferrous materials in sliding contact. An example of a bronze wear particle is illustrated in figure 14. It was the result of high cage wear in a ball bearing during a fatigue test (ref. 13).

## Grinding Particles

Spherical particles may also be produced by grinding operations (ref. 15). In the optical microscope these spheres appear quite similar to spheres related to rolling element fatigue. However, they are usually larger in diameter ( $>10\ \mu\text{m}$ ). Examination of these spheres is an SEM (fig. 15) reveals that many are hollow and their surface features, both internal and external indicate that a melting and resolidification process occurred.

## Cavitation Erosion Particles

Cavitation erosion has also been reported (ref. 11) to produce spherical particles. As in the case of the grinding spheres, they are normally  $>10\ \mu\text{m}$ . An example of a sphere isolated from a vane pump fluid in which cavitation erosion had occurred is shown in figure 16.

## Lubricant Breakdown Particles

Some lubricants under sliding contact conditions produce large quantities of an oil insoluble sludge like material. This material, which is often referred to as friction polymer, can clog filters, reduce clearances, and in general, reduce the life of the lubricant. An example of this type of debris is shown in figure 17. These particles were generated by a polyphenyl ether during boundary lubrication experiments (ref. 9). These particles are precipitated by the Ferrograph because they do contain some iron from the steel surface. Breakdown products that do not contain iron will not normally appear on a Ferrogram. However, these nonmagnetic particles can be precipitated by using magnetic ion solutions. Their use is described later.

## HYDRAULIC FLUID ANALYSIS

The types of wear particles described thus far are mainly associated with lubrication systems. However, these particles may also be produced in hydraulic systems. Many failures in industrial hydraulic systems are not predictable by wear particle monitoring alone. Organic debris in the hydraulic fluid may be indicative of seal or gasket failure.

Normally, this nonmagnetic organic debris will not be precipitated by the Ferrograph. However, the use of magnetizing solutions (ref. 17) which contains rare earth salts can effect precipitation. An example of the use of these solutions is shown in figure 18. In figure 18(a), the percent area covered by debris at various Ferrogram positions for the standard system

and the magnetizing system is shown for an initial hydraulic fluid sample. A little more debris is precipitated with the normal solution. However, data for a sample taken later from the same hydraulic system appears in figure 18(b). Now a large amount of additional debris appears with the magnetizing solution indicative of large amounts of organic debris in the sample. Subsequently, a hydraulic system failure occurred which was attributed to the failure of a fluoroelastomer seal.

## WEAR-TIME RELATIONSHIPS

### Wear Rate Versus Time

A generalized curve of wear rate, as a function of time appears in figure 19 (ref. 17). It shows the initial increase in wear rate associated with run-in or break-in, the low wear rate associated with the normal operating life and finally the higher wear rates reflecting wear out or failure.

### Wear Particle Distribution Versus Time

Figure 20 shows a generalized distribution of wear particles in the 2-5  $\mu\text{m}$ ; 15-25  $\mu\text{m}$  and total population during the three wear regimes. The quantity of wear particles is, of course, indicative of the prevailing wear rate. The amount of wear debris in the oil at any particular time can be determined from a Ferrogram by using the photodensitometer. Particle density readings can be made at different locations on a Ferrogram which will reflect the amount of large and small wear particles. A generalized ratio of large to small particles in each regime is shown in figure 21. This shows how changes in the ratio of large to small particles can be indicative of changes in wear mode.

## CONCLUDING REMARKS

It has been shown that the Ferrograph, in conjunction with an optical and a scanning electron microscope, can be used to determine various wear particle parameters. These include: quantity, size distribution, chemical composition, and morphology. Armed with this information one can accomplish the various levels of the health monitoring process. These are: detection, diagnosis, prognosis, and finally the prescription (fig. 22).

## ACKNOWLEDGEMENT

The author would like to thank M. Shibata and I. Shimizu of Mitsubishi Oil Company, LTD, Kawasaki City, Japan, for permission to use the photograph illustrating the cavitation erosion wear particle (fig. 16).

## REFERENCES

1. Ferrante, J.: Practical Applications of Surface Analytic Tools in Tribology. NASA TM-81484, 1980.

2. Kane, Philip F. and Larrabee, Graydon B., eds.: *Characterization of Solid Surfaces*. Plenum Press, 1974.
3. Davis, R.: *Rapid Response Instrumentation for Particle Size Analyses. A Review, Part One*, Amer. Lab., vol. 5, no. 12, Dec. 1973, pp. 17-23.
4. Burrows, J. A.; Heerdt, J. C.; and Willis, J. B.: *Determination of Wear Metals in Used Lubricating Oils by Atomic Absorption Spectrometry*. *Analyt. Chem.*, vol. 37, no. 4, Apr. 1965, pp. 579-582.
5. Kittinger, D. C.; and Bond, A.: *Spectrometric Analysis to Determine Wear Metal in Engine Lubricating Oil*. *Proceedings 18th Annual National Aerospace Electronics Conference*, May 16-18, 1966, IEEE, 1966, pp. 251-256.
6. Seifert, W. W.; and Westcott, V. C.: *A Method for the Study of Wear Particles in Lubricating Oil*. *Wear*, vol. 21, 1972, pp. 27-42.
7. Scott, D.; Seifert, W. W.; and Westcott, V. C.: *Ferrography - An Advanced Design Aid for the 80's*. *Wear*, vol. 34, 1975, pp. 251-260.
8. Jones, William R., Jr.; Nagaraj, H. S.; and Winer, Ward O.: *Ferrographic Analysis of Wear Debris Generated in a Sliding Elastohydrodynamic Contact*. *ASLE Trans.*, vol. 21, no. 3, 1978, pp. 181-190.
9. Jones, William R., Jr.: *Ferrographic Analysis of Wear Debris from Boundary Lubrication Experiments with a Five-Ring Polyphenyl Ether*. *ASLE Trans.*, vol. 18, no. 3, July 1975, pp. 153-162.
10. Reda, A. A.; Bowen, R.; and Westcott, V. C.: *Characteristics of Particles Generated at the Interface Between Sliding Steel Surfaces*. *Wear*, vol. 34, 1975, pp. 261-273.
11. Bowen, E. R.; and Westcott, V. C.: *Wear Particle Atlas. Final Report Contract N00156-74-C1682*, Naval Air Engineering Center, July 1976.
12. Scott, D.; and Mills, G. H.: *Spherical Debris - Its Occurrence, Formation and Significance in Rolling Contact Fatigue*. *Wear*, vol. 24, 1973, pp. 235-242.
13. Jones, William R., Jr.; and Stuart H. Loewenthal: *Analysis of Wear Debris from Full-Scale Bearing Fatigue Tests Using the Ferrograph*. *ASLE Trans.*, vol. 24, no. 3, July 1981, pp. 323-330.
14. Jones, William R., Jr.; and Parker, Richard J.: *Ferrographic Analysis of Wear Debris Generated in Accelerated Rolling Element Fatigue Tests*. *ASLE Trans.*, vol. 22, no. 1, Oct. 1977, pp. 37-45.
15. Jones, W. R., Jr.: *Spherical Artifacts on Ferrograms*. *Wear*, vol. 37, 1976, pp. 193-195.
16. Bowen, E. R.; and Anderson, D. P.: *Ferrographic Analysis of Acqueous/Glycol Type Lubricants and Hydraulic Fluids*, presented at the 36th National Conference on Fluid Power, Oct. 28-30, 1980, Cleveland, OH, pp. 199-204. (Illinois Institute of Technology is publisher.)
17. O'Donnell, P. M.: *Sample Preparation/Ferrogram Procedure/Ferrogram Analysis*. NAEC-MISC-92-0458, Naval Air Engineering Center, Aug. 1980.



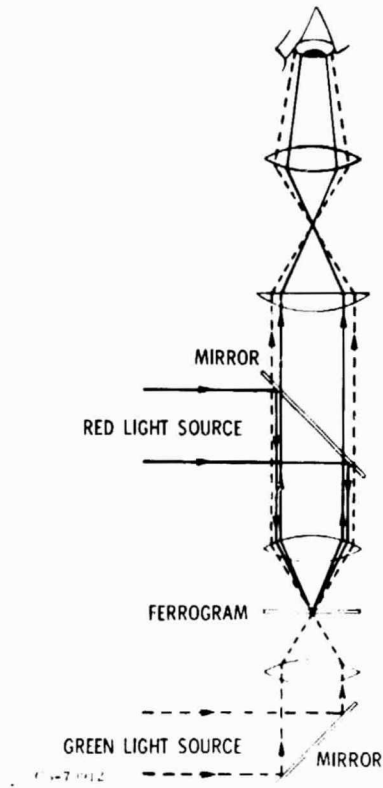


Figure 1. - Bichromatic microscope illumination system.

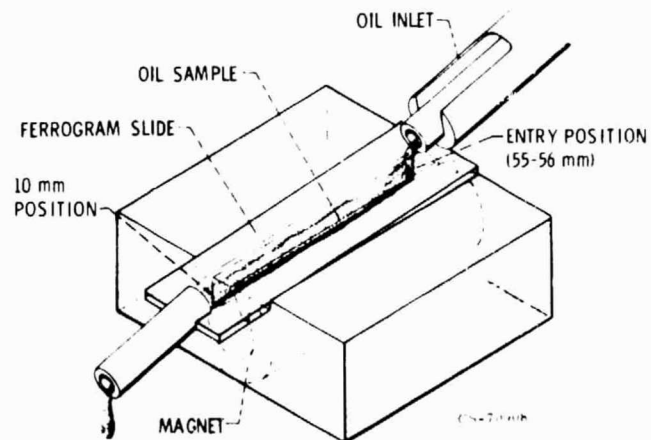
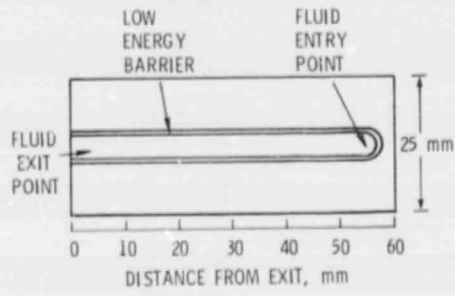


Figure 2. - Ferrograph analyzer.

ORIGINAL PAGE IS  
OF POOR QUALITY



CS-R1-3408  
Figure 3. - Ferrogram slide.



Figure 4. - Normal rubbing wear particles (from ref. 8).

ORIGINAL PAGE IS  
OF POOR QUALITY

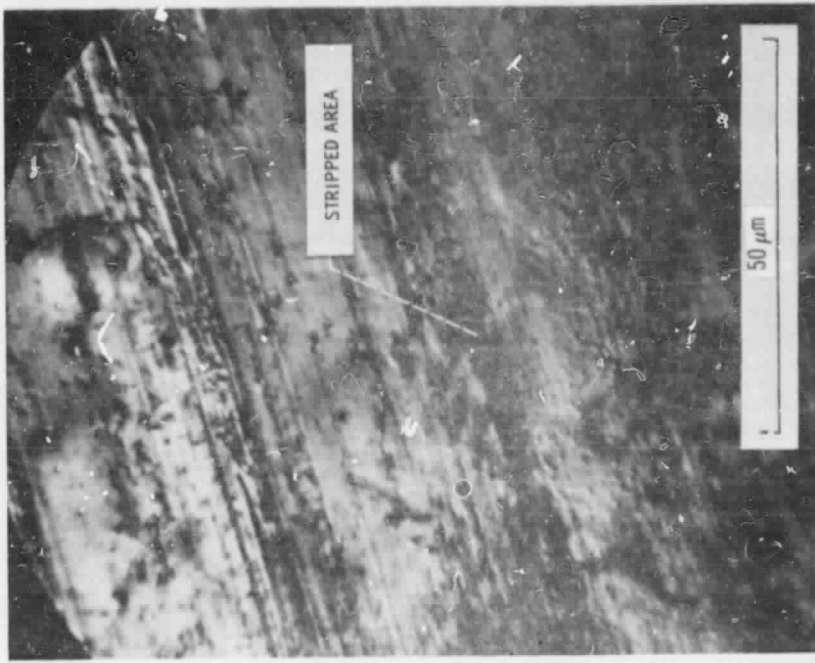


Figure 6. - Photomicrograph of wear scar obtained from interference contrast system. Lubricant, polyphenyl ether; specimen material, M-50 steel (from ref. 9).

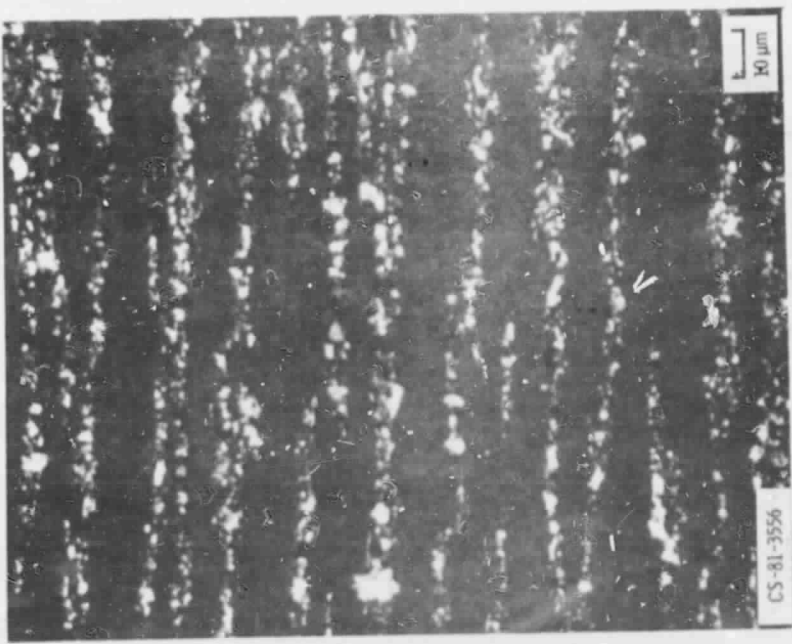


Figure 5. - Normal rubbing wear particle strings.

ORIGINAL PAGE IS  
OF POOR QUALITY



Figure 7. - Abrasive wear debris (from ref. 9).

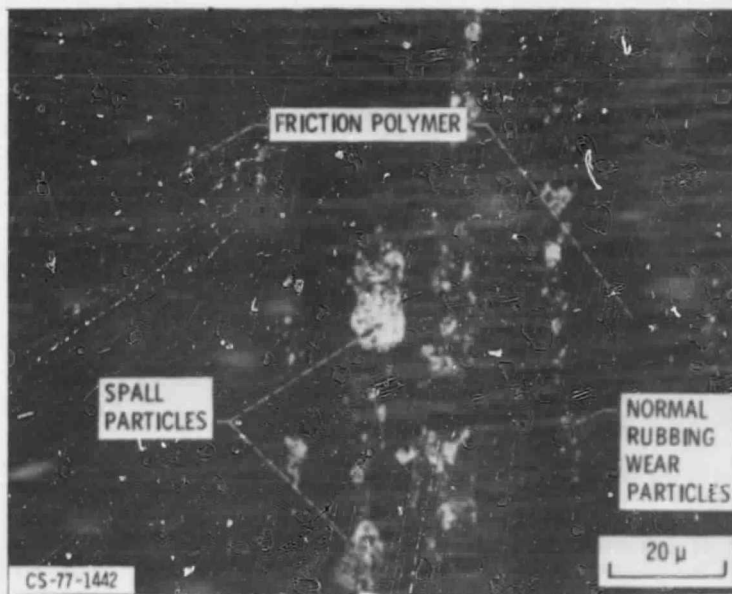


Figure 8. - Ferrogram entry deposit from bearing fatigue test (from ref. 14).

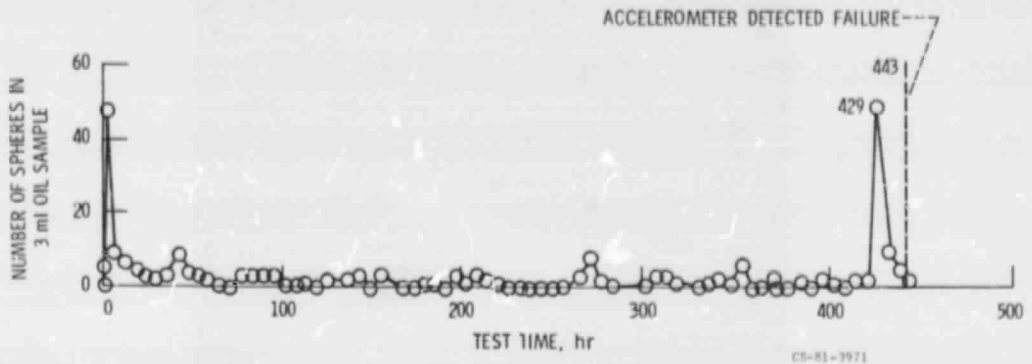


Figure 9. - Number of spheres in 3 ml of oil for full scale bearing fatigue test (from ref. 13).

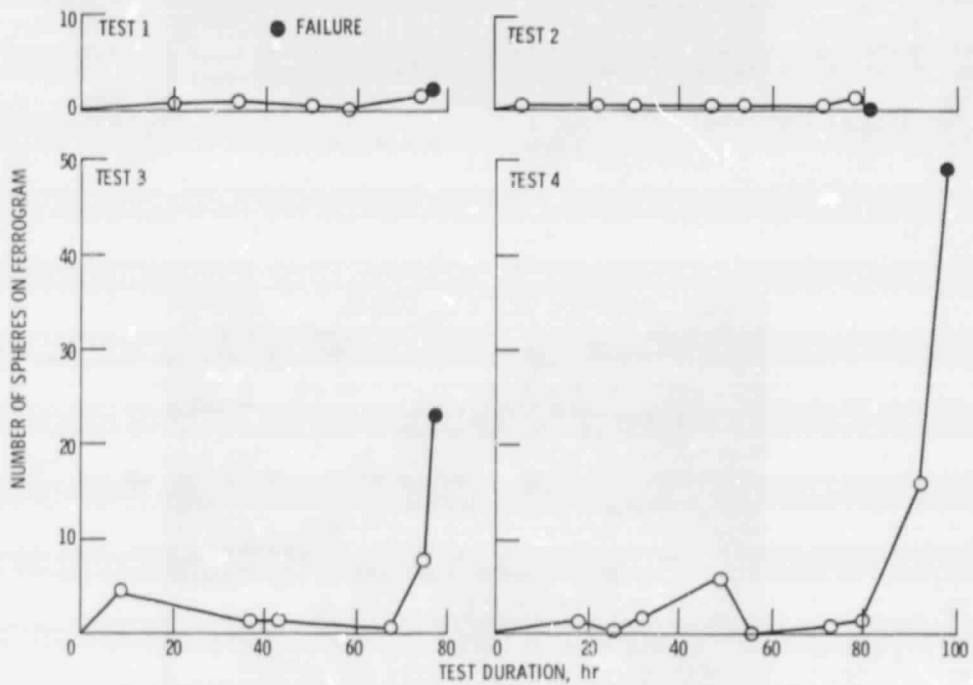


Figure 10. - Number of spheres on ferrogram as function of test duration for four fatigue tests (3 ml oil sample).



Figure 11(a). - Electron micrograph of spherical particle from accelerated fatigue test and (b) energy dispersive X-ray analysis of sphere (from ref. 14).

ORIGINAL PAGE IS  
OF POOR QUALITY



Figure 12. - Severe wear particle.

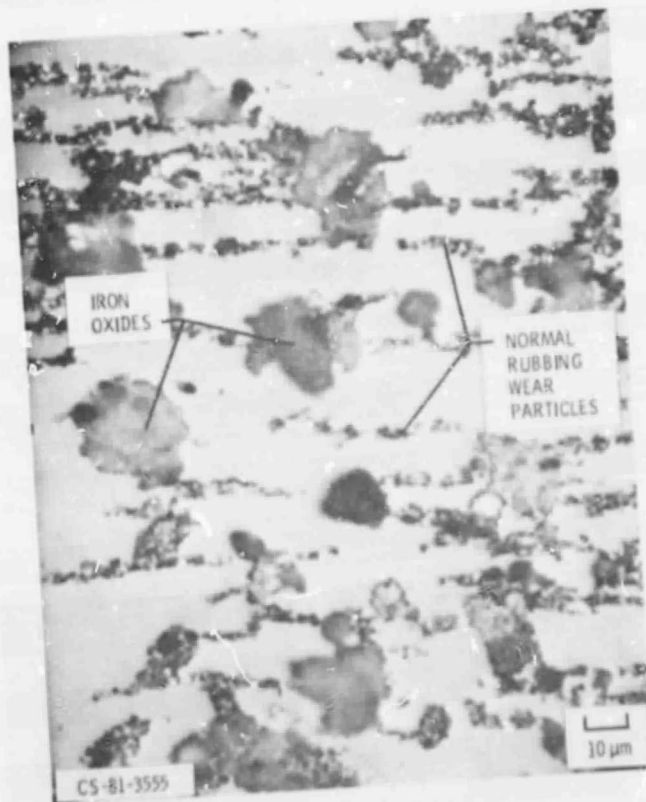


Figure 13. - Iron oxide debris.

ORIGINAL PAGE IS  
OF POOR QUALITY

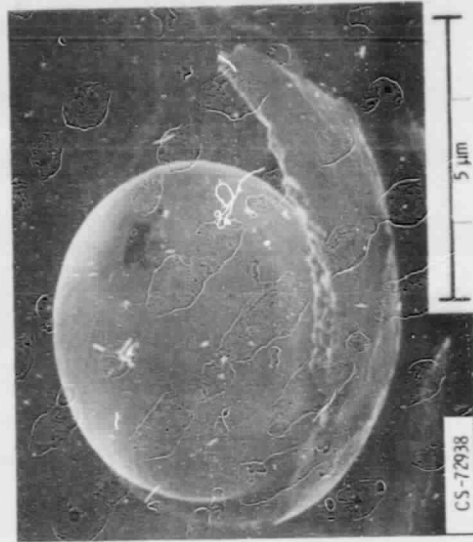
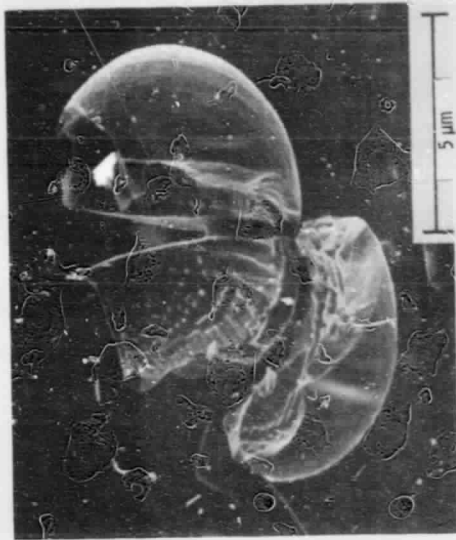


Figure 15. - Scanning electron micrographs of spherical grinding debris (from ref. 19).



Figure 14. - Bronze wear particle.

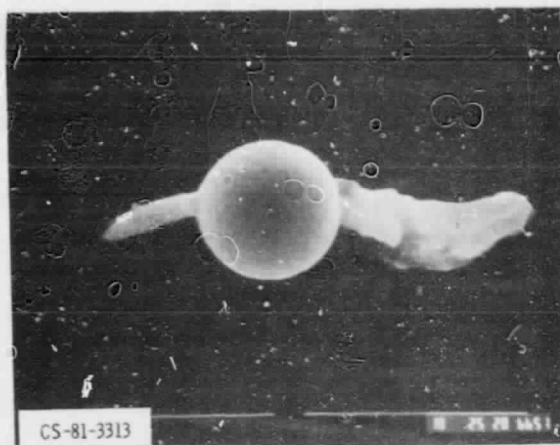


Figure 16. - Sphere produced by cavitation erosion.

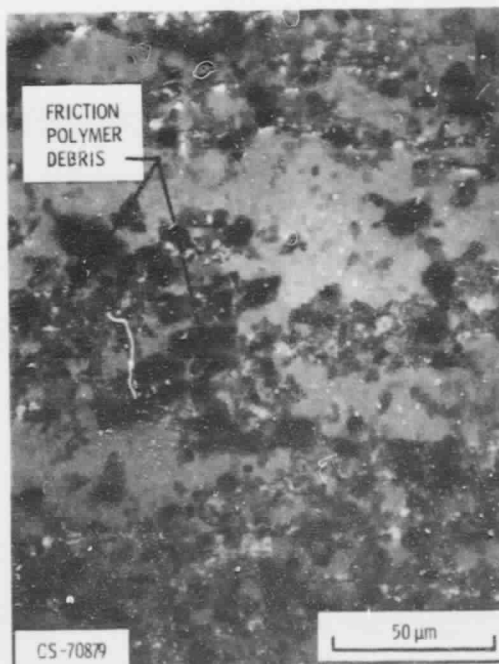


Figure 17. - Friction polymer wear debris (from ref. 9).



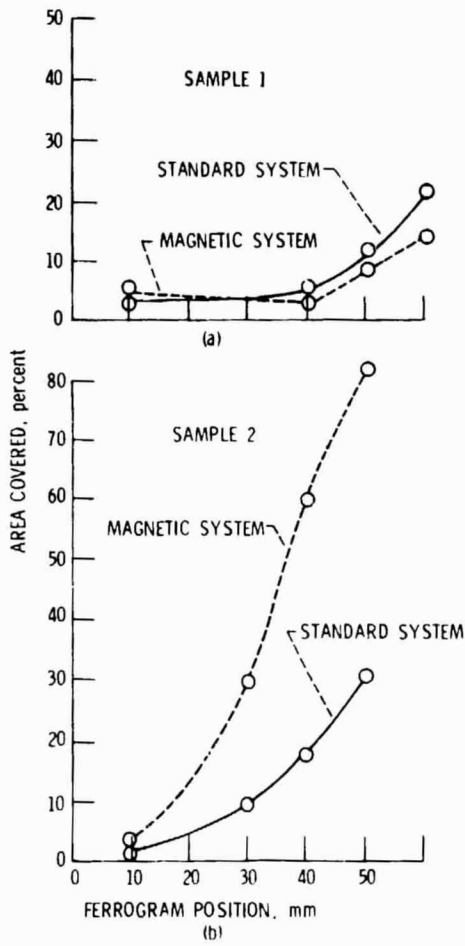


Figure 18. - Percent area covered at various ferrogram positions for (a) initial hydraulic fluid sample and (b) subsequent hydraulic fluid sample.

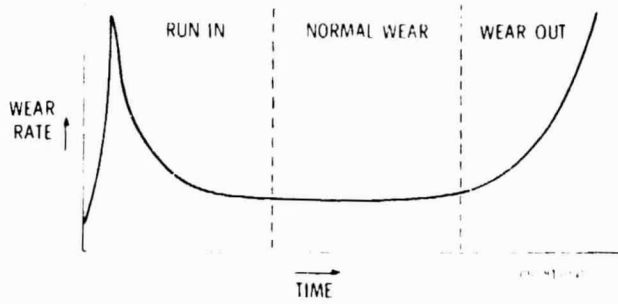


Figure 19. - Wear rate as a function of time (from ref. 17).

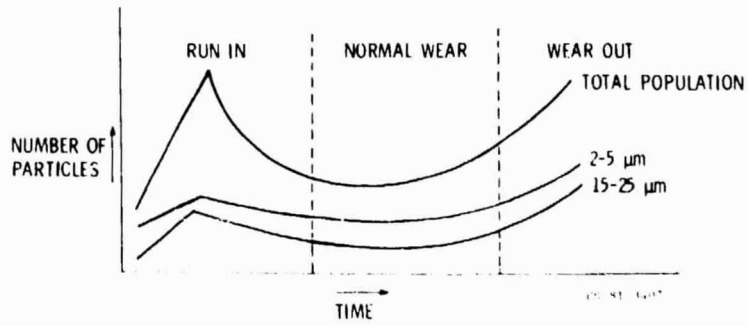


Figure 20. - Number of wear particles as a function of time (from ref. 17).

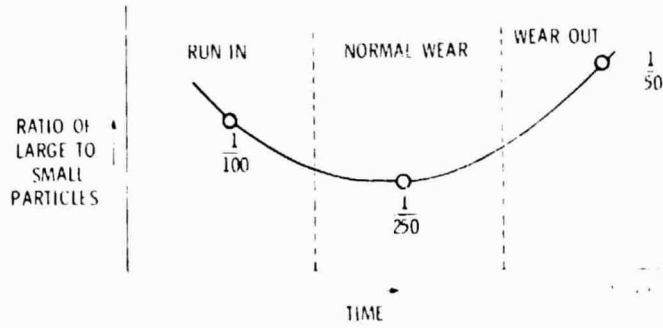


Figure 21. Ratio of large to small particles as a function of time (from ref. 17).

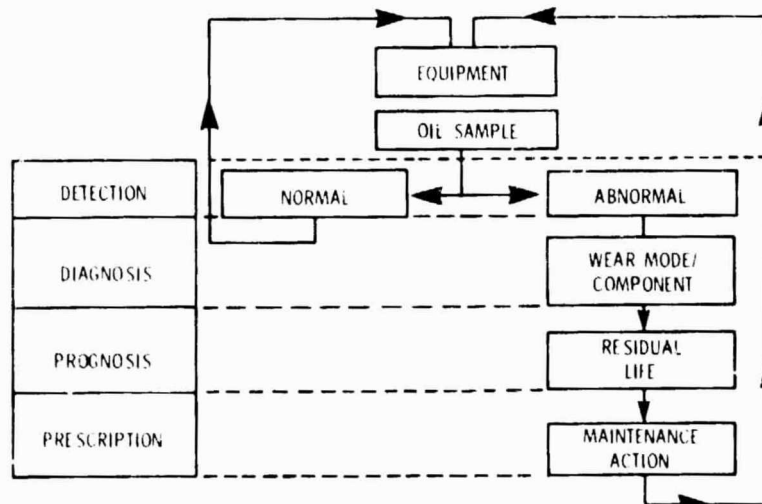


Figure 22. - Wear particle analysis, health monitoring process.